European Polymer Journal 221 (2024) 113525

Contents lists available at ScienceDirect

European Polymer Journal

journal homepage: www.elsevier.com/locate/europolj

Schiff base approach to introduce chitosan-phytic acid complex for flame-retardant cotton fabrics

Xiao-Mei Yang [a,b], Guang-Zhong Yin [c,d,**], Jose Hobson [d], Zhongjie Zhai [b], Junhuan Zhao [b,*], Baoqing Shentu [a,*]

[a] College of Chemical and Biological Engineering, Zhejiang University, Hangzhou 310027, China
[b] Zhejiang Ruico Advanced Material Co., Ltd., Huzhou 313018, Zhejiang Province, China
[c] Escuela Politécnica Superior, Universidad Francisco de Vitoria, Ctra. Pozuelo-Majadahonda Km 1.800, 28223 Pozuelo de Alarcón, Madrid, Spain
[d] IMDEA Materials Institute, C/ Eric Kandel, 2, 28906 Getafe, Madrid, Spain

ARTICLE INFO

Keywords:
Flame retardant
Sustainable polymers
Cotton fabric
Chitosan-phytic acid complex
Surface functionalization

ABSTRACT

In this study, chitosan was integrated onto cotton fabric fibers through a Schiff base reaction, followed by the in-situ generation of Chitosan-Phytic acid (CH-PA) complex to achieve green flame retardancy. The process began with oxidizing the fabric using sodium periodate ($NaIO_4$) to create numerous aldehyde groups on the fiber surface. Subsequently, CH was grafted onto the fabric via a Schiff base reaction. The fabric was then immersed in a PA solution to form a CH-PA complex, resulting in a novel and highly efficient flame-retardant (FR) fabric. The structure of the treated fabric was analyzed by using Fourier-transform infrared spectroscopy (FTIR), Scanning electron microscopy (SEM), and energy-dispersive spectroscopy (EDS), confirming the successful formation of the desired structure. The thermal stability and flame retardancy of the fabric were systematically evaluated using thermogravimetric analysis (TGA), cone calorimetry (CONE), vertical combustion tests, and limiting oxygen index (LOI) measurements. The LOI increased from 17.6 % to 30.6 %, and vertical combustion tests demonstrated self-extinguishing capabilities when the fabric was treated by the $NaIO_4$ solution at concentrations of 0.02 g/mL or higher. In the CONE test, the modified fabric showed significant improvements, with peak heat release rate (pHRR) and total heat release (THR) decreasing by approximately 80 % and 60 %, respectively. Comprehensive analysis indicated that the FR mechanism involved both gas phase and condensed phase actions. Further characterization of the material included tensile testing and wash resistance assessments. By comparing these findings with recent research on similar topics, the advantages and disadvantages of the materials were thoroughly evaluated. Notably, this work provides a robust experimental foundation and conceptual expansion for the green flame retardancy of cotton fabrics.

1. Introduction

In the realm of textile engineering, the quest for flame retardant (FR) materials that are both effective and sustainable has emerged as a paramount challenge. Amidst this pursuit, cotton, renowned for its comfort, breathability, and widespread application across various industries, stands as a cornerstone of the textile industry. Studies have extensively documented the environmental consequences of conventional FR treatments on cotton textiles [1]. Recent research has focused on exploring alternative FR agents and eco-friendly application methods to address the sustainability concerns associated with conventional treatments. Bio-based additives, such as CH [2,3] and lignin [4,5], have shown promise in enhancing flame retardancy while minimizing environmental impact. Additionally, advancements in nanotechnology have enabled the development of nanostructured coatings and functionalized nanoparticles for efficient FR delivery on cotton fabrics [6]. The literature highlights the urgent need for sustainable strategies in FR cotton fabric production. Through the exploration of alternative materials, innovative technologies, and holistic approaches to environmental stewardship, the textile industry can mitigate the ecological footprint of

* Corresponding authors.
** Corresponding author at: Escuela Politécnica Superior, Universidad Francisco de Vitoria, Ctra. Pozuelo-Majadahonda Km 1.800, 28223 Pozuelo de Alarcón, Madrid, Spain.
E-mail address: amos.guangzhong@ufv.es (G.-Z. Yin).

https://doi.org/10.1016/j.eurpolymj.2024.113525
Received 25 June 2024; Received in revised form 24 August 2024; Accepted 23 October 2024
Available online 26 October 2024

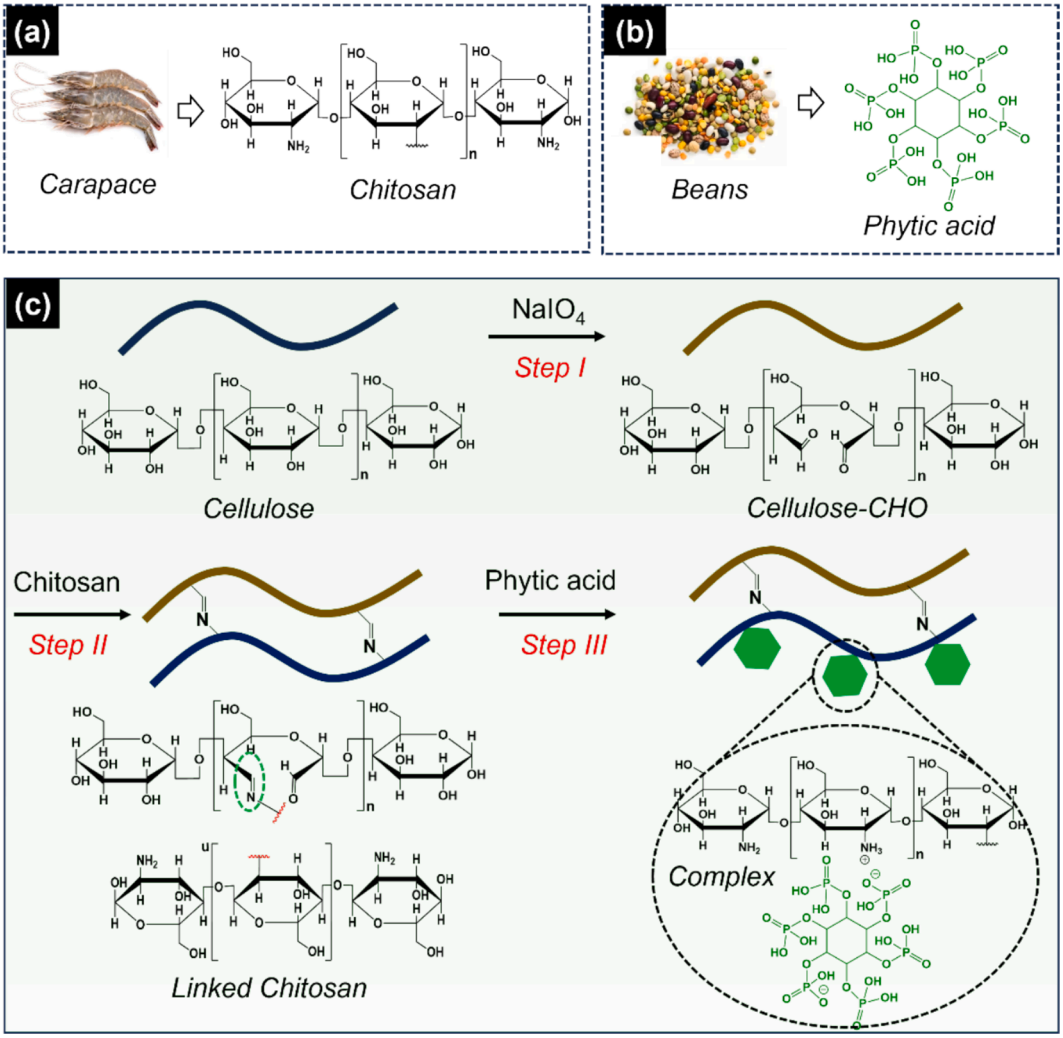

Fig. 1. (a) The significant sources and chemical formula of CH, (b) the main sources and chemical formula of PA, and (c) the process of FR fabric: (Step I) $NaIO_4$ oxidation to prepare cellulose fabric with aldehyde groups; (Step II) Schiff base formation, introducing CH onto the fabric through chemical pathway; (Step III) PA introduction by forming the CH-PA complex.

FR treatments while ensuring safety, comfort, and performance.

The Chitosan-Phytic acid (CH-PA) complex is a widely researched and applied green FR. One application strategy involves first synthesizing the CH-PA complex, then using it as a FR in the preparation of composite materials [7,8]. For example, Sun *et al.*, [9] presents a facile preparation of FR, and reinforced poly(lactic acid) (PLA) composite using CH-PA complex. The thermal and burning properties of PLA composites were evaluated by thermogravimetric analysis (TGA), limited oxygen index (LOI), UL-94, and cone calorimetry. PLA/CH-PA showed earlier mass loss and higher char residue than pristine PLA. CTSPA (3 wt%) enhanced the LOI value of PLA from 19.6 % to 30.5 % and achieved V-0 ratings in UL-94 test. The second strategy is to utilize layer-by-layer (LbL) self-assembly [10], or dip coating [11,12], for the surface modification of foam [13] or fabrics [14,15]. For example, Fang *et al.* constructed multifunctional coating on cotton fabrics through LbL assembly strategy by using PA and CH, and spraying copper ion and polydimethylsiloxane, anticipating endowing them with flame retardancy and superhydrophobic properties. The coated cotton fabric achieved a LOI value of 32 %, revealing excellent flame retardancy [3]. They further reported a FR cotton fabrics, which were also prepared by LbL coating consisting CH and PA, and both carbon nanotubes (CNTs) and graphene oxide (GO). The PA-GO/CSCNTs coated cotton fabric showed excellent flame retardancy with a LOI of 31 %, and could self-extinguish rapidly after removing the flame [16]. LbL self-assembly with PA and CH was widely applied for the fabric surface functionalization. As reported, the complexes might release NH_3, which is nonflammable, in the thermal degradation process to dilute the concentration of flammable gases [17]. However, fabrics treated with LbL self-assembly or finishing solutions often have high loading, which can affect the fabric's flexibility and breathability. To achieve surface modification conveniently and efficiently, chemical grafting may be a better option.

Schiff bases are widely applied in dynamic self-healing hydrogels [18–20], as well as in recyclable epoxy resins, among other areas. Specifically, Klein et al. [21] use vanillin aldehyde derivatives as monomers, which are further cured with bio-based di- and triamines, leads to covalent adaptable Schiff base networks and thus enables sustainable and thermally reprocessable high-performance materials. By systematically adjusting the composition of the network building blocks, the mechanical properties could be varied from tough materials with a high elastic modulus of 1.6 GPa. The combination of bio-based building blocks and the degradability of Schiff base networks under acidic conditions resulted in sustainable and recyclable with self-healing properties. In Zamani *et al.*'s recent study [22], a multifunctional vanillin-based monomer was synthesized, and it can be cured using a diamine without any organic solvent. A carbon fiber reinforced polymer (CFRP) was fabricated using Schiff base polymer through the compression molding technique. Its mechanical and fire performance were compared

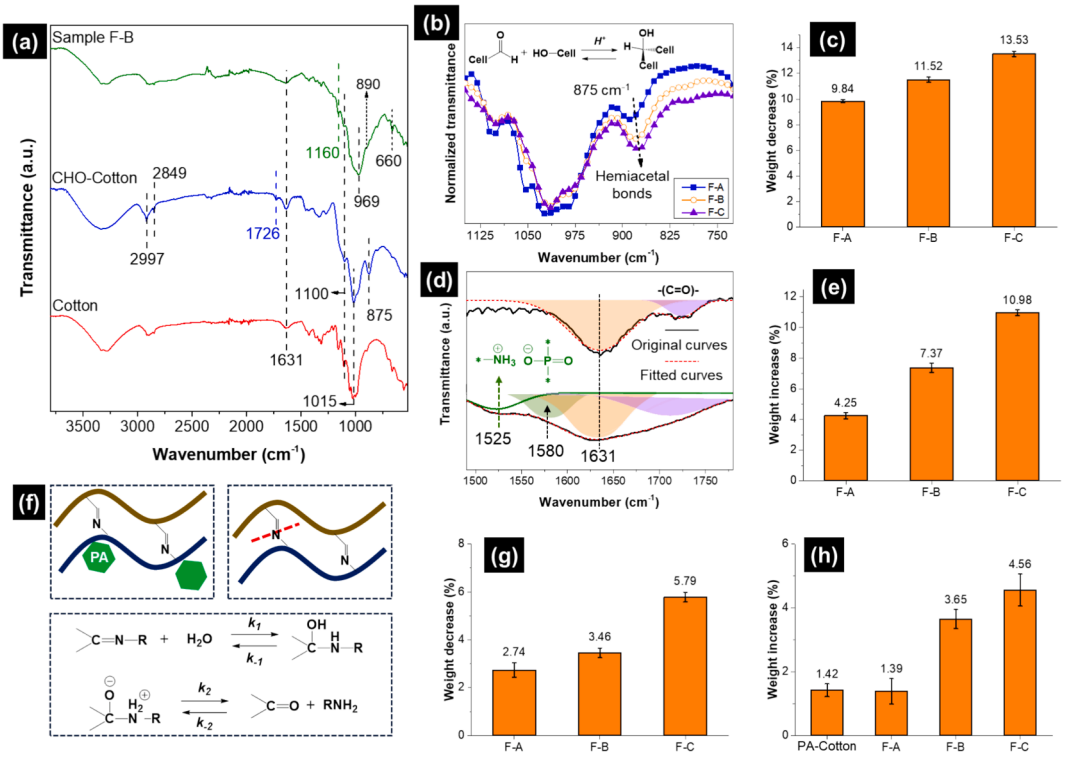

Fig. 2. (a) FTIR plots of typically samples: cotton (control sample), CHO-cotton and the final product F-B, (b) FTIR spectra of three samples (CHO-Cotton for sample F-A, CHO-Cotton for sample F-B, and CHO-Cotton for sample F-C) in the specific range of 725–1150 cm^{-1}, (c) Mass change during the sample fabrication process: weight loss during $NaIO_4$ treatment, (d) FTIR information of samples CHO-Cotton (top) and F-B (bottom) in the range of 1500–1750 cm^{-1}, (e) Mass variation after introducing CH onto the sample, (f) Schematic of Schiff base degradation process, [23,24] and analysis of the reasons for the final decrease in mass under PA treatment, (g) Mass variation after introducing PA into the sample, and (h) weight increase as FR loading ratio.

to a CFRP made from a commercially available grade epoxy resin. The resulting Schiff based CFRP composite demonstrated exceptional fire retardancy, and along with impressive tensile strength and Young's modulus. In a brief summary, the Schiff base method is widely used in the design and preparation of recyclable thermosetting polymer materials due to its efficiency and reversibility.

Above all, this work embarks on a comprehensive exploration of sustainable strategies for enhancing the flame retardancy of cotton fabric. We aim to achieve FR modification of cotton fabric using green chemicals efficiently and to systematically evaluate the advantages and disadvantages of this system, providing comprehensive insights and materials for the relevant field. Specifically, (1) Using $NaIO_4$ oxidation to release aldehyde groups on cotton fiber, enabling the Schiff base reaction; (2) Employing the mild Schiff base reaction to graft CH at the molecular level onto the fiber surface for efficient coating; and (3) utilizing the widely applied CH-PA complex system to achieve efficient flame retardancy for cotton fabric.

2. Results and discussion

2.1. FR fabric fabrication and structure confirmation

Fig. 1 illustrates the schematic diagram of the FR cotton fabrics preparation process. We selected CH and PA as the core modifying agents (Fig. 1a, Fig. 1b). The specific modification process is depicted in Fig. 1c. We oxidized the surface of the fabric fibers with $NaIO_4$, expecting to release an appropriate amount of aldehyde groups (Step I), as further depicted in **Figure S1**. We introduced CH onto the fabric surface in a chemically bonded form by utilizing Schiff base, followed by the reaction between CH and PA to form the CH-PA complex (Fig. 1c, Step III). The preparation process and the experimental details are provided in Section S1. The detailed parameters of the series of samples are listed in **Table S1**. For comparison, we selected samples treated with PA alone (PA-Cotton) and untreated samples (sample control) as references, sample PA-Cotton (**Figure S2**). We characterized typical samples using FTIR spectroscopy, aiming to confirm the success of the reactions, as shown in Fig. 2a.

The characteristic signals of all the samples are in the region of 3000–3500 cm^{-1} corresponded to the stretching O–H groups [25], ~1100, ~970, and 1726 cm^{-1} are assigned to the vibrational stretching P═O groups in phosphate, bending P-H, and C═O, respectively [26]. The bands are observed near 1631 cm^{-1} correspond to the O–H stretching and bending vibration of water molecules adsorbed on the surface of the fibers [27]. The spectra of pure CH (**Figure S3**) exhibited its characteristic peaks at 1060 cm^{-1} and 660 cm^{-1}, we therefore compare and attribute the signals at corresponding positions in the modified samples to CH. Other detailed signal attributions are listed in **Table S2**. Notably, the appearance of band at 875 cm^{-1} is due to the formation of hemiacetal bonds between the aldehyde groups and neighboring hydroxyl groups, as shown in Fig. 2**b** inset. FTIR spectra show new IR band at ~875 cm^{-1} and the intensities of these bands increase noticeably when increasing $NaIO_4$ concentration, which to a certain extent indicates the proportion of aldehyde group formation (oxidation) increasing. The appearance of characteristic peak at about 1726 cm^{-1} also confirm the formation of aldehyde products [28]. As shown in **Figure S4**, the hydroxyl peaks weaken with increasing oxidation levels. This is mainly because many hydroxyl groups have been converted into aldehyde groups, leading to a weakening of the hydroxyl bonding to some extent. The occurrence and extent of oxidation reactions can also be reflected by Fig. 2**c**. Typically, there is a decrease in the mass of the $NaIO_4$ treated cotton fabrics, with F-A, F-B, and F-C experiencing decreases of 9.84 %, 11.52 %, and 13.53 %, respectively. This indicates that the higher the oxidation level, the more significant the loss in mass. After the formation of aldehyde groups, two

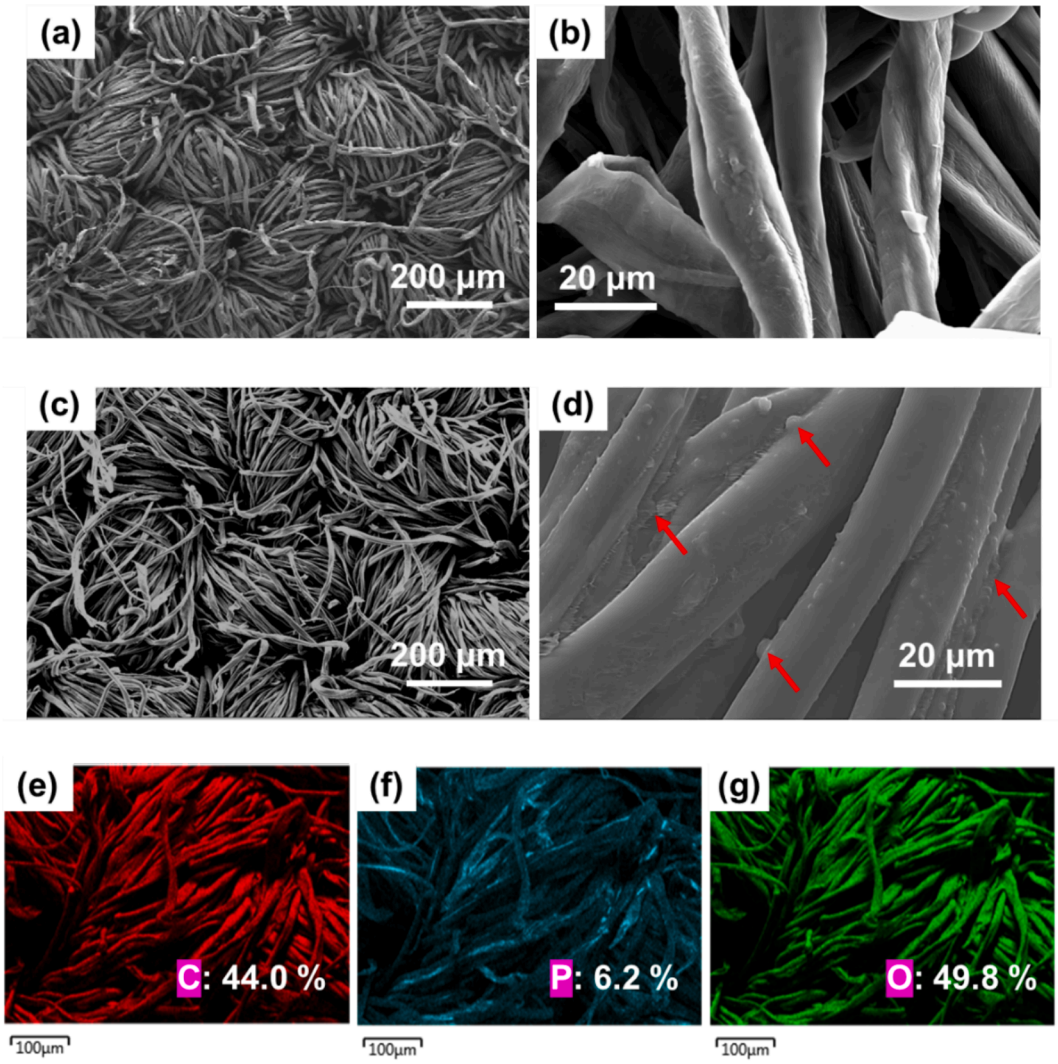

Fig. 3. (a) and (b), SEM images of control cotton; (c) and (d), SEM images of sample F-B; and EDS images of sample F-B: (e) C, (f) P and (g) O (N is not sensitive to be detected) and the elements content according to the EDS test.

medium-intensity absorption peaks appeared in the range of 2880–2650 cm^{-1}, with similar intensities and relatively sharp profiles, which are characteristic spectral bands of aldehyde groups (Fig. 2a and Figure S4).

The FTIR spectrum of cellulose Schiff base displayed significant absorption bands at 1580 cm^{-1} for C═N [23]. It overlaps with the peak of adsorbed water at 1631 cm^{-1}, forming a broad peak, as shown in Fig. 2**d**. The signal at 1525 cm^{-1}, which can be assigned to the NH_3^+ vibration, as the characteristic signal of group $–NH_3^+$-(O-(P═O)═)-, which is indicating ionic complexation between protonated CH and negatively charged PA [7,29,30]. The results and analysis indicated that the reactions between CH and PA occurred successfully. Compared with the spectrum of control sample, the functionalized sample showed the new bands at 1160 and 1050 cm^{-1} belonging to the stretching vibration of P═O and O-P-C structures of PA. The signals of CH are difficult to be clearly distinguished from those of cotton fabric due to some similar structures between cotton and CH chain [14].

As shown in Fig. 2**e**, the masses of F-A, F-B, and F-C increased by 4.25 %, 7.37 %, and 10.98 %, respectively. This increase is believed to be proportional to the contents of CH present on the fabric surface. It correlates positively with the extent of oxidation of the fabric fibers by $NaIO_4$. However, when the samples were subsequently reacted with PA at room temperature for two hours, a decrease in mass was observed. As illustrated in Fig. 2**f**, we assigned the possible reasons for the weight decrease. Schiff base can undergo hydrolysis under acidic conditions, meaning that during the formation of the PA-CH complex, Schiff base may undergo some degree of hydrolysis, leading to the detachment of CH chains. The combined results led to a decrease in mass, with reductions of 2.74 %, 3.46 %, and 5.79 % for F-A, F-B, and F-C, respectively (Fig. 2**g**). Compared to the CHO-Cotton, the mass of final functionalized samples increased. Specifically, the mass increases for F-A, F-B, and F-C were 1.39 %, 3.65 %, and 4.56 %, respectively, corresponding to the weight gain index of FR, as shown in Fig. 2**h**.

After the modification, the appearance of the fabric did not undergo significant changes. Only those with excessively high oxidation levels may look slight yellow. There was no significant change in softness. We conducted SEM characterization on typical samples, namely control cotton and sample F-B, and the results are shown in Fig. 3**a-d**. The control fiber surface appears smooth, while the modified surface shows some roughness, with protrusions as shown by the red arrows in Fig. 3**d**. We attribute this roughness to the grafted CH-PA complex. Despite the presence of the complex, there was no significant change in fiber diameter. We also performed EDS spectrum characterization on the samples (Fig. 3**e-g**), which revealed the presence of a large amount of phosphorus (P) elements, likely originating from the PA in the complex. Here, we cannot deny the possibility of PA reacting directly with hydroxyl groups on the fabric. However, the small amount of PA present in this manner does not affect our primary analysis of the material components [31,32]. By employing EDS and SEM, and based on the

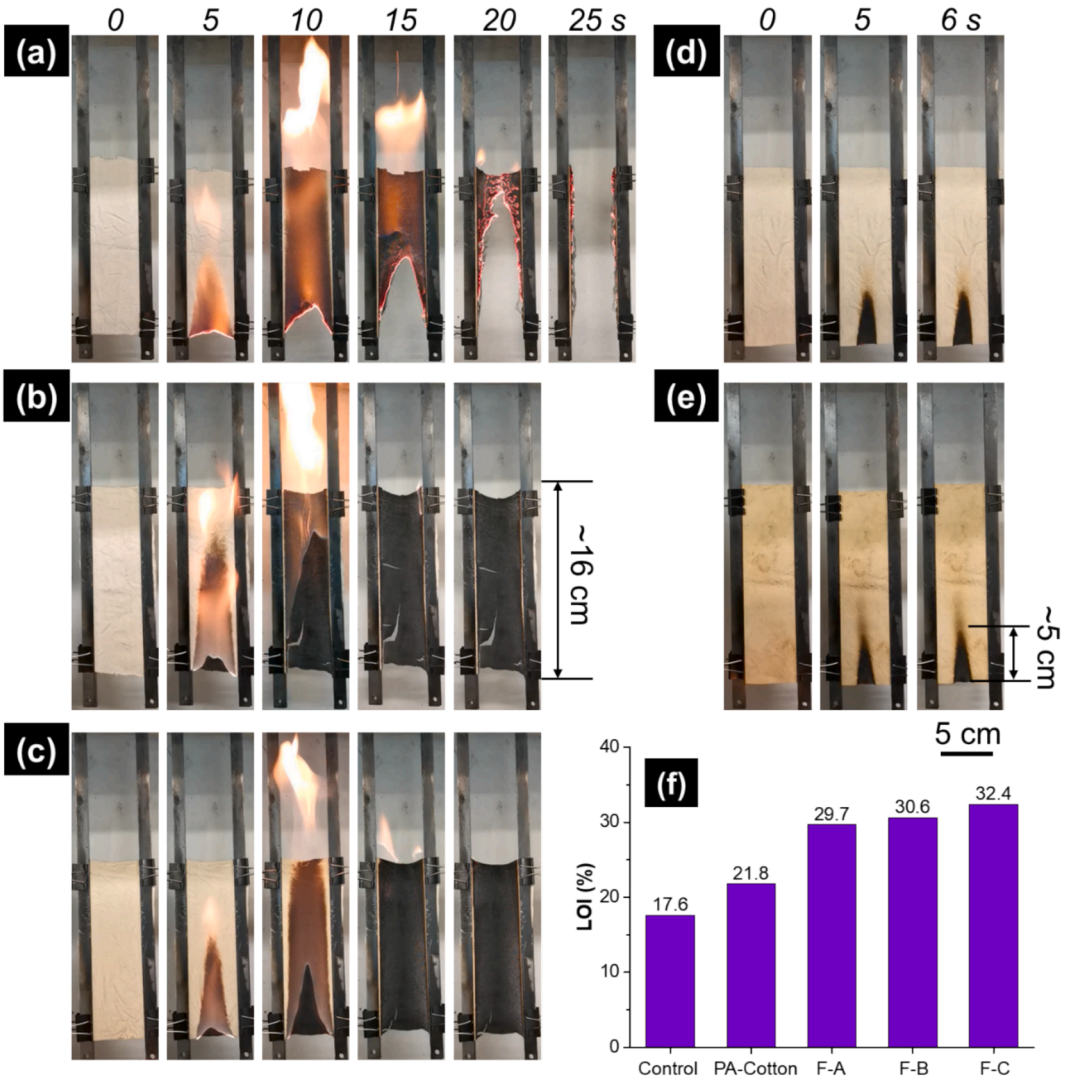

Fig. 4. Digital photos of cotton samples in vertical flame test after 5 s: (a) cotton control fabric, (b) PA modified, (c) F-A, (d) F-B, (e) F-C, and (f) LOI values of all samples.

aforementioned findings, it was visually confirmed that a certain amount of CH-PA complex was introduced onto the fabric surface through chemical bonding.

2.2. Fire safety characterization

2.2.1. Vertical combustion test

The vertical burning test of the fabric visually reveals the differences in burning before and after modification, as well as the differences in samples obtained from different modification processes. As shown in Fig. 4a, the control sample burns completely within 25 s, with almost no residual char remaining. However, all samples modified with both PA and PA-CH complex show significantly improved charring properties. Samples PA-Cotton and F-A fail to achieve self-extinguishment. Nevertheless, they exhibit high charring and no afterglow phenomenon (Fig. 4b and 4c). Additionally, we observe that samples containing the complex at the same loading exhibit better continuity of char layer (no cracks) compared to PA-Cotton. The synergistic FR effect of the complex results in better charring properties. When the concentration of $NaIO_4$ treatment is above 0.02 g/mL, the material achieves self-extinguishment (Fig. 4d and 4e). Through the LOI index reaction, its LOI can increase from the original 17.6 % to above 32.4 % (Fig. 4f).

2.2.2. CONE calorimeter

To fully understand the fire safety of the F-B, CCT was used, and the results were shown in Fig. 5 and the corresponding data were listed in Table 1. The peak of heat release rate (pHRR) for F-B reduced by 80 % in contrast with that of control fabric. Total heat release (THR) for F-B decreased by 60 % from 9.2 MJ/m^2 of cotton to 3.8 MJ/m^2. This improvement caused by synergistic effect of N in CH and phosphorus from PA in FR system, as also explored by reports elsewhere [33,34]. The weight loss rate of F-B has been declining significantly in comparison with cotton, seen in Fig. 5c. In Table 1, the char residue of F-B (39.1 %) remarkably increased from 5.6 % of control fabric, which was well depicted in TGA analysis. The control sample was almost consumed after CCT while F-B maintained their shapes in image of Fig. 5f. A sharp increment for total smoke production (TSP) value after functionalization, which can be attributed to the incomplete combustion of the functionalized samples [35,36]. The residue of F-B maintained the cotton structure and cellulose integrity. Notably, as showed in Fig. 5g, the formation of bubbles, being trapped in the swelling residue, to some extent proved the presence of intumescent char layer.

2.2.3. Flame retardancy mechanism analysis

The char morphologies of the F-B before and after combustion were detected by SEM, as shown in Fig. 6, to further explore the mechanism of

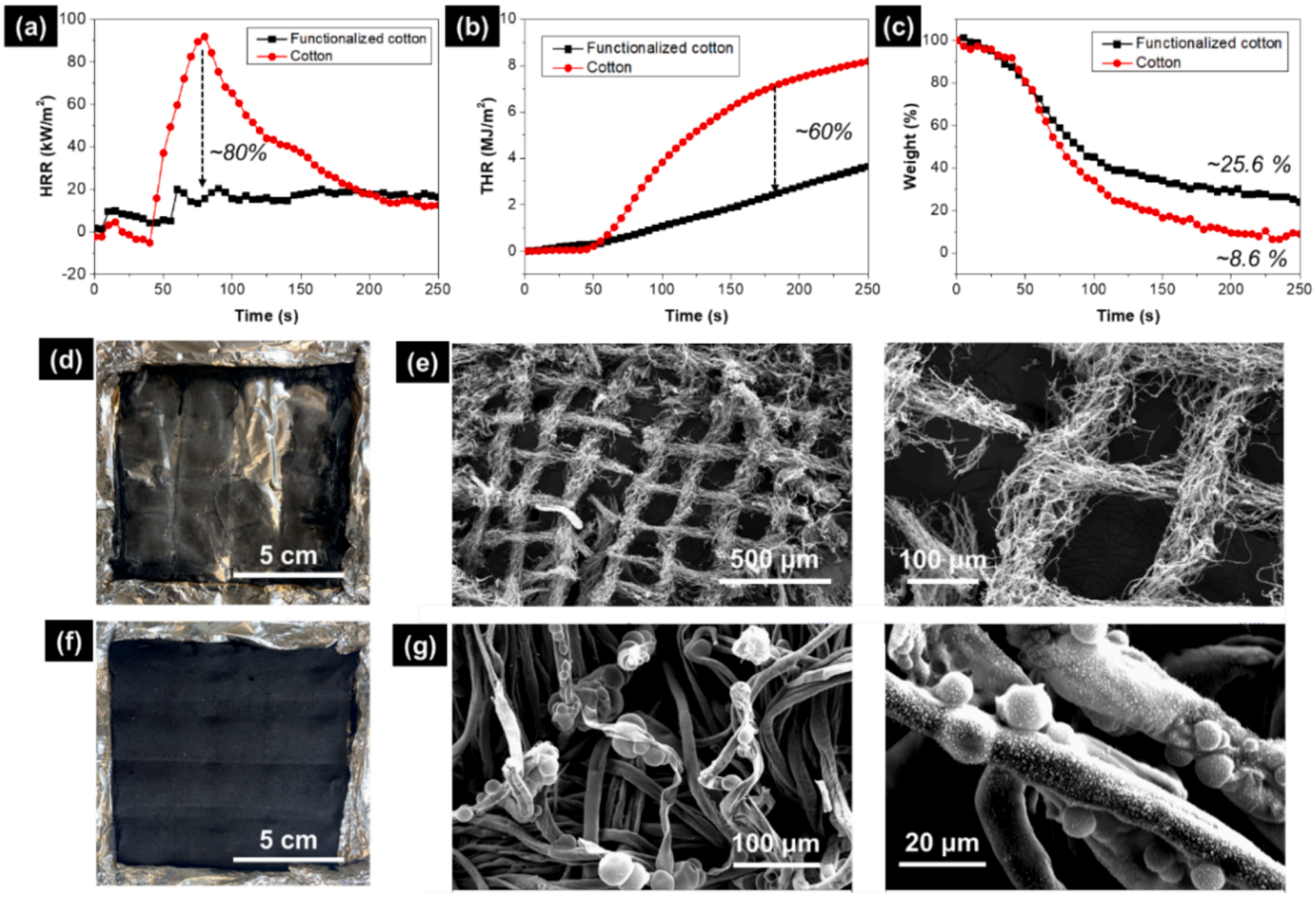

Fig. 5. (a) HRR curves, (b) THR curves of Cotton (Control sample) and F-B, (c) weight loss curves, (d) digital photo of cotton residue after CCT, (e) SEM images of the char residues of cotton sample after the CONE test, (f) digital photo of F-B residue after CCT, and (g) SEM images of the residues of sample F-B after CONE test.

Table 1
Parameters obtained by CONE calorimeter.

Samples	pHRR (kW/m^2)	THR (MJ/m^2)	Mass remaining (%)	Smoke production (m^2)
F-B	21 ± 1	3.8 ± 0.5	25.1	0.38 ± 0.03
Control	113 ± 15	9.2 ± 0.6	5.6	0

synergistic flame retardancy between cotton fabric and PA-CH complex. The SEM results of the modified samples are shown in Fig. 6a. Microscopically, the fibers exhibit certain striping, as indicated by the red outlined area in Fig. 6a, which is consistent with the schematic representation. After burning in the air, it is evident that the fibers appear more rounded overall, with many bubbles appearing, as shown in the red box in Fig. 6b. Additionally, the average diameter of the fibers before burning is approximately 13.76 μm, while after burning, the average diameter of the fibers increases significantly, to approximately 16.21 μm. This may be because during combustion, the FR undergoes thermal gasification, leading to a certain degree of expansion in the fiber matrix itself. Combining the analysis of the results in Fig. 5g and Fig. 6 with numerous reports on similar FR systems suggests that gas-phase flame retardancy plays a very important role in the FR process. Therefore, as shown in Fig. 6b, some bubbles were formed, resulting from the escape of non-flammable gases produced during the decomposition of the functionalized fabric.

We then performed EDS characterization on another set of modified samples, and the results are shown in Fig. 7. Firstly, after combustion, the proportion of carbon (C) in the samples significantly increased. For specific elemental content results, please refer to **Figure S6**. The proportion of phosphorus (P) also increased significantly. Specifically, for sample F-B, the P content increased from 6.2 % before combustion (as shown in Fig. 3f) to 9.4 % after combustion. Additionally, we found that the P element was evenly distributed, and the fiber morphology could be well maintained for all samples F-A, F-B and F-C. As the FR loading increased, the P content increased, and the same trend was observed for oxygen (O) (Fig. 7h). This indicates to a certain extent that the oxygen in the material exists in the form of phosphate ions. The carbon source from cotton fibers, the gas source mainly from CH, and the acid source from PA together achieve efficient flame retardancy in a trinity manner.

Based on the above discussion, the possible FR mechanisms are proposed, as illustrated in Fig. 8. By the combination of PA-CH complex, the FR system can form a network structure of chemical crosslinking in the cotton fabric matrix and impart FR action in both the gas and condensed phase. In detail, PA is first degraded to generate phosphoric acid, which works as an acidic catalyst. Moreover, the phosphoric acid possibly promotes the crosslinking and condensation of both cellulose and CH molecules and improve char strength. At the same time, due to a large amount of phosphorus (P species) in PA, free radical scavengers are produced during the combustion process to stop the combustion reaction [37]. Simultaneously, non-combustible gases such as CO_2, H_2O, and NH_3 (N specias) released from the CH molecules contained in the PA-CH complex can dilute the concentration of fuel gas to reduce combustion intensity. In the condensed phase, an intumescent layer composed of P-containing thermostable structures formed as a good physical barrier. In this FR system, PA can perform as an acid source, generating polyphosphoric acid during the combustion or decomposition, which dehydrated cotton and promoted the carbonization. NH_3 from CH as blowing

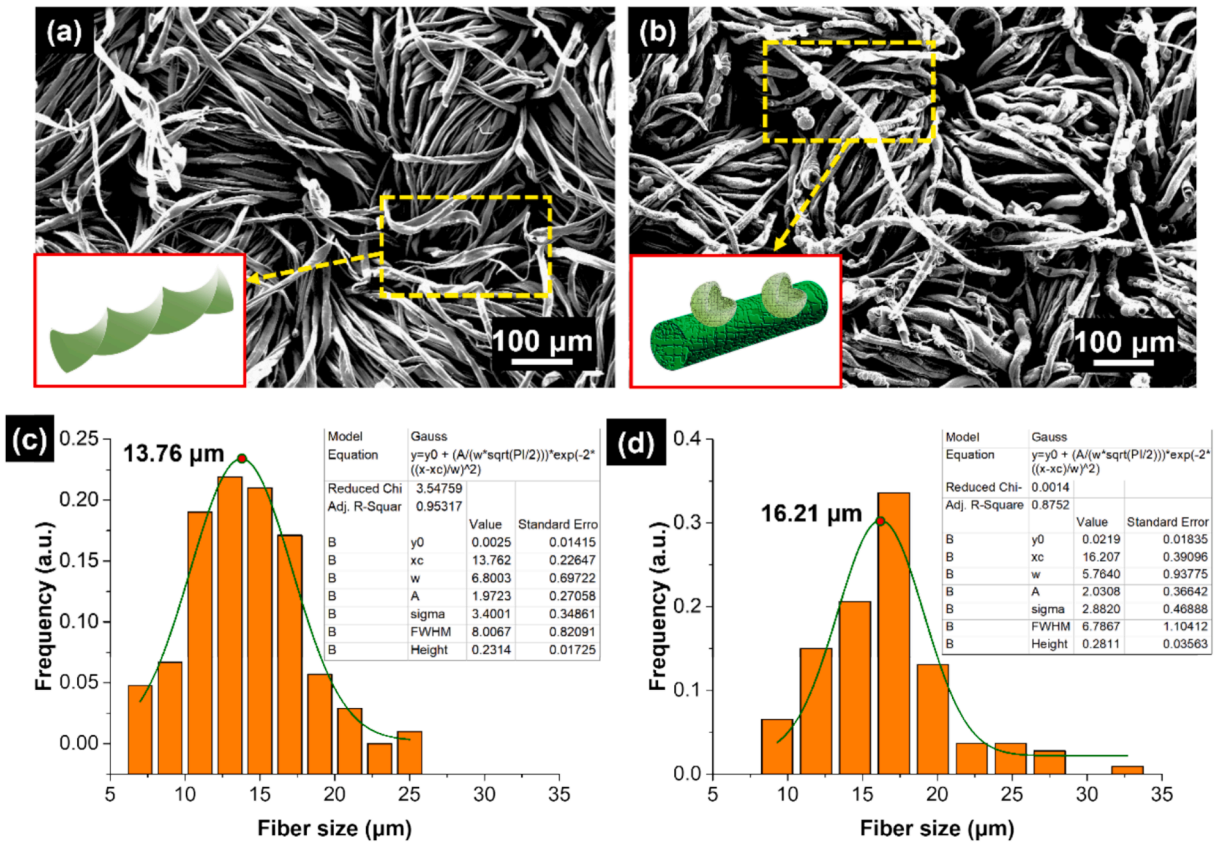

Fig. 6. (a) SEM image of sample F-B, (b) char SEM image of sample F-B, (c) diameter and distribution of the fiber and (d) the diameter and distribution of char for sample F-B.

agent can dilute the combustible gas. The cellulose and CH units could work as carbon source. Therefore, the flame is inhibited by the synergistic action of CH-PA interrupting the free radical chain reaction and considerably improving the flame retardancy of cotton fabric.

2.3. Stability

2.3.1. Thermal stability

The TG and DTG curves are depicted in Fig. 9. The corresponding data are listed in Table 2. As shown in Fig. 9a, mass loss around 100 degrees Celsius results from the evaporation of adsorbed water. The main weight loss of the control ranges from 250 to 400 °C, exhibiting the T_{max} at 350.56 °C. The main reason for this phenomenon is due to the depolymerization of cellulose. Compared with the control sample, FR cotton fabrics present lower T10% values. Extraordinarily, as the increased mass elevated, $T_{10\%}$ of FR cotton fabrics reduced gradually. It is well reported PA may produce phosphoric acid and polyphosphoric acid during the degradation, and can catalyze the thermal degradation process of cellulose, leading to lower $T_{10\%}$ values [38]. It can be further observed from Fig. 9 and Table 2 that the values of Tmax of FR cotton fabrics are also lower. The T_{max} values of F-A, F-B, and F-C are 286.56, 288.27, and 291.82 °C, respectively. The char residual amounts at 700 °C are significantly improved from 7.28 % (control) to 31.29 % (F-A), 32.78 % (F-B), and 38.23 % (F-C). It is because PA can catalyze the dehydration and carbonization reactions of cellulose, resulting in the formation of more char residues, as well reported in the literature elsewhere [39].

2.3.2. Mechanical performance and brief durability evaluation

Due to the low loading of FRs, there have been no significant changes in fiber diameter and morphology. Therefore, the fabric exhibits excellent softness, almost resembling the original fiber fabric. The tensile test results are presented in Fig. 10. The tensile strength was 9.4 (± 2.3) MPa and the elongation at break is 13.5 (± 1.7). After functionalization, the tensile strength and elongation decreased to 4.9 (± 0.8), and 10.4 (± 1.5), respectively. A slight decrease in elongation at break can be observed, while the tensile strength decreases significantly, remaining at around 50 % of the original sample. As shown in Table 3, it is evident that a decline in mechanical properties is a common result of the cotton fabric modification. We can briefly infer the main reasons for the mechanical decline. Namely, during the oxidation process, fiber molecules are eroded to a certain extent, and after oxidation, some hydroxyl groups are converted to aldehyde groups, leading to a decrease in intermolecular hydrogen bond density. Additionally, in aqueous solutions and acidic environments, water induces moderate degradation of cellulose, as illustrated in Fig. 10d. Both of these factors contribute to molecular chain breakage and a decrease in local supportiveness. Additionally, after washing for 5 min, the fabric mass decreased by 1.74 (0.5)%. The LOI decreased to 26.4. As shown in Fig. 10e, the FR performance of the fabric was significantly weakened, with no self-extinguishing phenomenon observed. Fortunately, its charring ability is still well preserved.

2.4. Analysis of advantages and disadvantages

Overall, this is a convenient and efficient FR strategy. It demonstrates typical advantages and significant improvements in FR performance and processing. Efficient flame retardancy can be achieved with ultra-low FR loading. As shown in Table 3, the amount added in many references ranges from 10 wt% to 45 wt%. After modification, the material's texture undergoes no significant change. Under certain controlled conditions, such as sample F-B, the color consistency can be maintained to the naked eye, as shown in Fig. 4a. However, this system also has significant flaws and shortcomings:

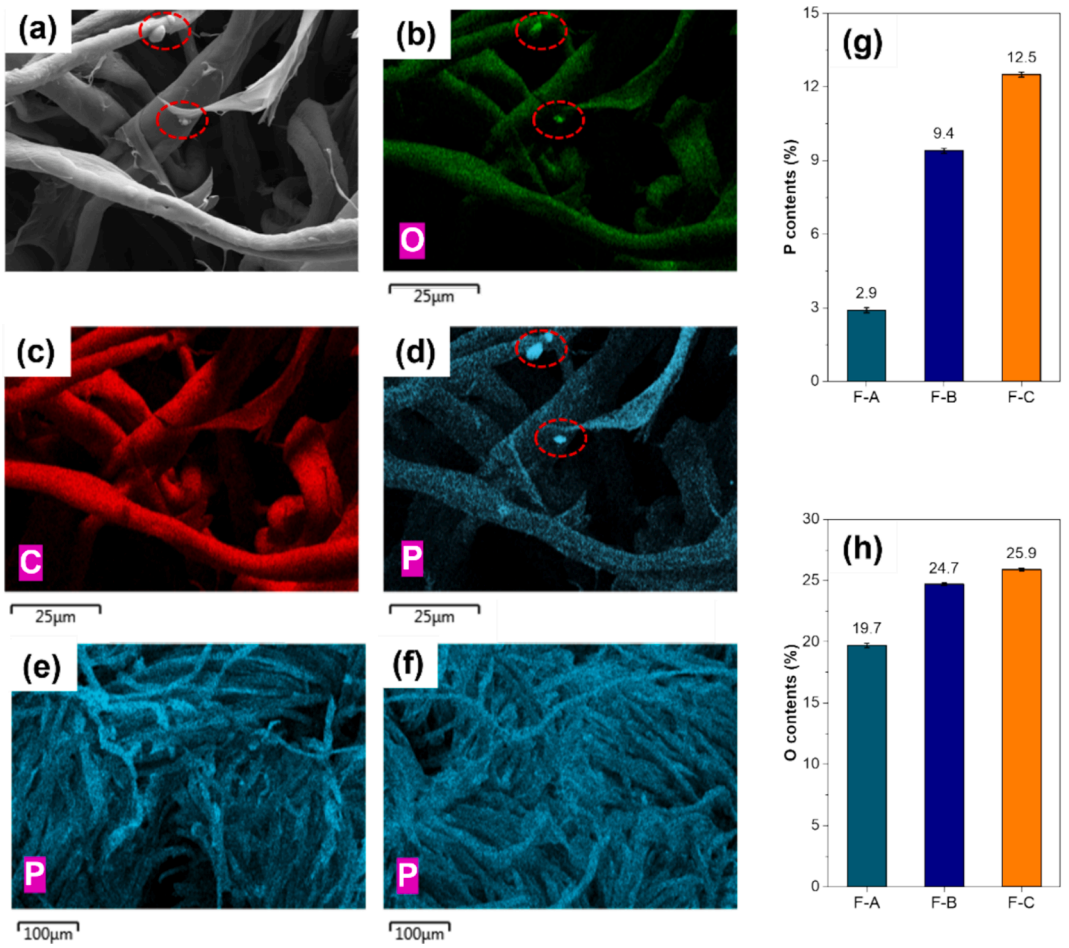

Fig. 7. Comparison of Phosphorus content in residual carbon. (a) SEM image of sample F-A, (b) EDS image for O element of sample F-A, (c) EDS for C of sample F-A, (d) EDS for P of sample F-A, (e) EDS image for P of sample F-B, (f) EDS image for P of sample F-C, (g) P contents based the EDS test, and (h) the oxygen ratio based on the EDS results.

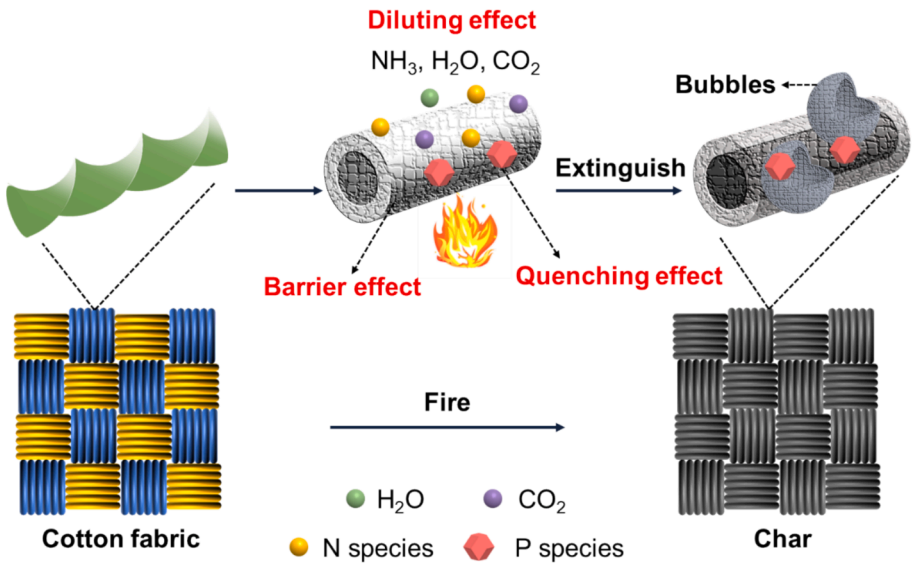

Fig. 8. Proposed FR mechanisms, which is combined effect of gas phase (Diluting effect) and condensed phase (Barrier effect).

Significant decrease in mechanical performance, a common issue in other cotton fabric modification systems (Table 3). One of the advantages of this method is that the softness and texture of the modified material do not change significantly. However, the tensile strength is decreased significantly.

We also conducted preliminary tests on the wash resistance of the samples. Handwashing with pure water for 5 min at room

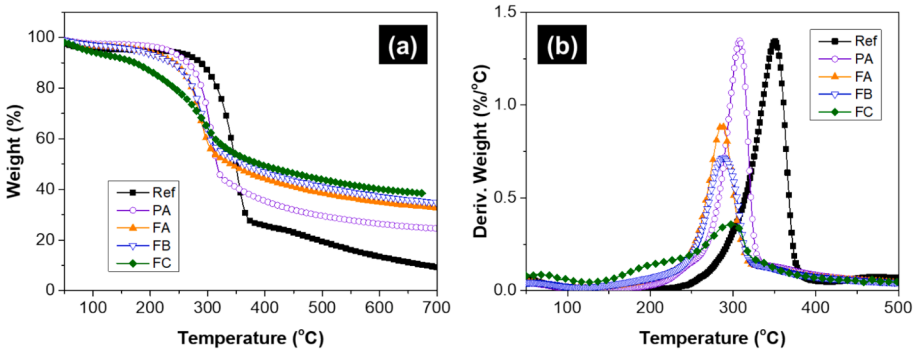

Fig. 9. TGA results: (a) TGA curves and (b) DTG curves of sample control, PA-cotton, F-A, F-B and F-C.

Table 2
Typical parameters obtained from TGA test.

Sample	Water release (%)	$T_{10\%}$ (°C)	T_{max} (°C)	Char (%) at 700 °C	R_{max} (%/°C)
Control	4.26	288.07	350.56	7.28	1.36
PA-Cotton	2.64	264.93	308.00	23.58	1.35
F-A	3.11	241.56	286.56	31.21	0.90
F-B	2.65	237.88	288.27	32.78	0.73
F-C	7.00	172.56	291.82	38.23	0.36

Note: $T_{10\%}$ means the temperature at which 90% weight remain.

temperature, significantly decreases the fabric's flame self-extinguishing performance, as shown in Fig. 10e. The LOI decreases to 26.4 %. This may be due to the overall instability of the phosphite in an acidic environment in water. Therefore, the suitable application scenario for this modified fabric should be dry conditions, with non-repeated washing requirements.

Further work could focus on refining the material preparation process, such as achieving the minimum treatment time, in the meantime self-extinguishing and the minimum concentration of $NaIO_4$, the shortest time for PA treatment at room temperature, aiming to achieve high mechanical performance retention, self-extinguishing, and high efficiency of FR loading in FR cotton fabrics.

3. Conclusion

A FR coating composed of CH and PA was successfully deposited on cotton fabric by Schiff base method. The flame-retardancy of cotton fabric is remarkably improved. Compared with pristine cotton fabric, the LOI of sample F-B which is treated by the $NaIO_4$ solution with concentration of 0.02 g/mL reaches as high as 30.6 %, achieving self-extinguishing performance. The pHRR and THR of F-B were reduced by about 80 % and 60 %, respectively. The CH-PA complex coating improves fire safety in cotton fabric due to two key factors, which the release of nonflammable N-containing gases in the gas phase. In the condensed phase, the formed carbon layer catalyzed by PA is thermally stable enough to insulate the entry of oxygen and heat. We observed a

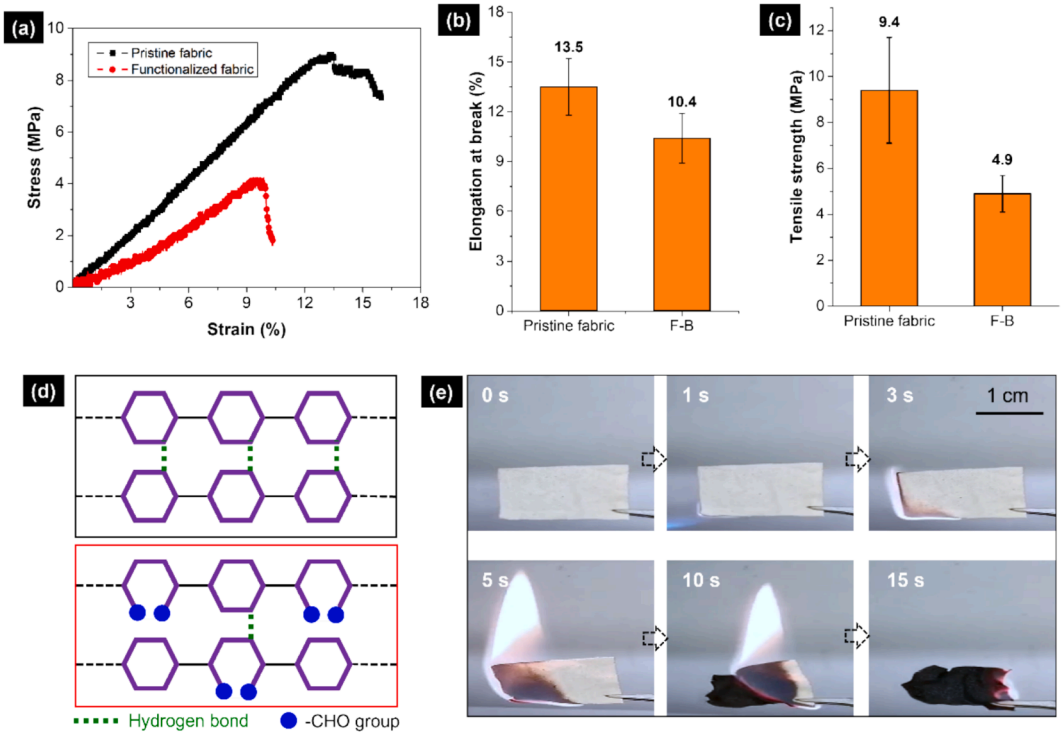

Fig. 10. (a) Stress-Strain curves of pristine fabric and the F-B, (b) Elongation at break results, (c) Tensile strength of pristine fabric and the F-B, (d) illustration for the possible degradation of cellulose in acidic environments, and (e) the fire performance after washing.

Table 3
Comparison and Analysis of Parameters in FR Modification of Cotton Fabrics Compared to Others.

No.	Cotton fabric information	FR strategies	FR composition	FR loading ratio (%)	Duration and temperature (h)	pHRR decrease (%) (Heat flux)	LOI (%)	Mechanical strength change (%)	Self-extinguished	Ref.
1		LbL	lignosulfonate and CH	17.1–25.2	< 1h	16.5 (35 kW/m^2)	24.7–26	−19.5 warp; −18.0 weft	Yes	[40]
2		FR molecule to the fiber through a strong P–O–C bond	glycerol, phosphoric acid, and urea	25.3	–	91.2 (Not giving)	40.5	Remained in the usable range	Yes	[41]
3		Crosslinking reaction between cotton fibers and APA	PA, urea, Dicyandiamide	20.0	110 °C, 170 °C	–	43.2	−24.4	–	[42]
4		Three steps, TA (super high concentration)	tannin (TA), tartar emetic (TE), and Fe^{2+}	29.0	60 °C	27.4 (35 kW/m^2)	27.0	–32.1	Surviving from the test	[43]
5		Hydrolysis and condensation of TEOS; Curing with APP; dipping in SA	APP, tetraethoxysilane (TEOS), sodium alginate (SA)	10 wt%	70–75 °C	63.6–81.7 (35 kW/m^2)	19–31.0	−8.4	Yes	[44]
6			Formaldehyde, Phosphorous acid, Triethylenetetramine, urea, dicyandiamide	8.7–35.5	95 °C, 2 h for the FR; 60 °C, 20 min, twice for impregnation	89.6 (35 kW/m^2)	26–40.9	−25.1	Yes	[45]
7			$NH_4H_2PO_4$, urea, melamine	25.4	135, 10 min; 60, 2 h	70.11 (35 kW/m^2)	51.1	−10.75	Yes	[46]
8	Wool fabric	LbL	PA-CH	19.8	70 °C	39.0 (25 kW/m^2)	33.3	–	Yes	[14]
9	Cotton fabric	LbL deposition	PA, CH, and biochar	45.3	70 °C	88.7 (35 kW/m^2)	64.1	–	Yes	[47]
10	Cotton fabric	LbL	3-Aminopropyltriethoxysilane, phenylphosphonic acid, dopamine hydrochloride	33.6	80 °C	36.0 (25 kW/m^2)	31.4	+10	Yes	[37]
11		Chemical grafting-complexing, two steps	PA and CH	1.39–4.56	3 h, 3 h, 2 h Less than 50 °C	(25 kW/m^2)	21.8–32.4	−40	Yes	This work

significant increase in char formation and a noticeable decrease in thermal decomposition rate in the modified material, consistent with the results from the CONE test. Mechanical performance testing results indicate a decrease in tensile strength of the fabric after modification, primarily due to the oxidation-induced defects in cellulose chains and partial cellulose degradation. Notably, this study shows that CH-PA complex coating deposited on substrate by Schiff base reaction opens up an effective and eco-friendly way for current FR field.

CRediT authorship contribution statement

Xiao-Mei Yang: Writing – review & editing, Writing – original draft, Investigation, Formal analysis, Data curation. **Guang-Zhong Yin:** Writing – review & editing, Writing – original draft, Supervision, Resources, Project administration, Investigation, Funding acquisition, Formal analysis, Data curation, Conceptualization. **Jose Hobson:** Writing – review & editing, Formal analysis, Data curation. **Zhongjie Zhai:** Writing – review & editing, Data curation. **Junhuan Zhao:** Writing – review & editing, Supervision, Funding acquisition. **Baoqing Shentu:** Writing – review & editing, Supervision, Project administration.

Declaration of competing interest

The authors declare that they have no known competing financial interests or personal relationships that could have appeared to influence the work reported in this paper.

Acknowledgements

This work was partially supported by NEWSAFE (No.: PID2022-143324NA-I00) Projects funded by Ministerio de Ciencia, Innovación y Universidades (MICIU, Spain), and partially funded by Zhejiang Leading Innovation and Entrepreneurship Team (2022R01019).

Appendix A. Supplementary data

Supplementary data to this article can be found online at https://doi.org/10.1016/j.eurpolymj.2024.113525.

Data availability

No data was used for the research described in the article.

References

[1] J. Lu, Y. Zhang, Z. Jiang, Y. Wang, X. Chen, H. Zhang, K. Chen, S. Zhai, Y. Yu, D. Qi, Turn waste into treasure: novel high-efficiency, reactive, and Sericin-based intumescent flame retardant for cotton fabrics, ACS Sustain. Resource Manage. 1 (4) (2024) 694–706.
[2] Q. Fang, Y. Zhan, X. Chen, R. Wu, W. Zhang, Y. Wang, X. Wu, Y. He, J. Zhou, B. Yuan, A bio-based intumescent flame retardant with biomolecules functionalized ammonium polyphosphate enables polylactic acid with excellent flame retardancy, Eur. Polym. J. 177 (2022) 111479.
[3] Y. Fang, L. Chen, J.W.L. Liu, Multi-functionalization of cotton fabrics with excellent flame retardant, antibacterial and superhydrophobic properties, Int. J. Biol. Macromol. 254 (2024) 127889.
[4] B. Kassaun, P. Fatehi, Solvent-free lignin-silsesquioxane wood coating formulation with superhydrophobic and flame-retardant functionalities, Chem. Eng. J. 493 (2024) 152582.

[5] M. Li, M.N. Prabaker, J.-I. Song, Effect of synthesized lignin-based flame retardant liquid on the flame retardancy and mechanical properties of cotton textiles, Ind Crops Products 212 (2024).
[6] L. Zhang, Z. Li, D.-Y. Wang, Polydopamine-assisted strategies for preparation of fire-safe polymeric materials: a review, Eur. Polym. J. 138 (2020) 109973.
[7] T. Zhang, H. Yan, L. Shen, Z. Fang, X. Zhang, J. Wang, B. Zhang, Chitosan/phytic acid polyelectrolyte complex: a green and renewable intumescent flame retardant system for ethylene-vinyl acetate copolymer, Ind. Eng. Chem. Res. 53 (49) (2014) 19199–19207.
[8] Y. Liu, A. Zhang, Y. Cheng, M. Li, Y. Cui, Z. Li, Recent advances in biomass phytic acid flame retardants, Polym. Test. 124 (2023) 108100.
[9] Y. Zhou, B. Tawiah, N. Noor, Z. Zhang, J. Sun, R.K.K. Yuen, B. Fei, A facile and sustainable approach for simultaneously flame retarded, UV protective and reinforced poly(lactic acid) composites using fully bio-based complexing couples, Compos. B Eng. 215 (2021) 108833.
[10] B. Wang, Y.-J. Xu, P. Li, F.-Q. Zhang, Y. Liu, P. Zhu, Flame-retardant polyester/cotton blend with phosphorus/nitrogen/silicon-containing nano-coating by layer-by-layer assembly, Appl. Surf. Sci. 509 (2020) 145323.
[11] P. Qi, S. Wang, W. Wang, J. Sun, H. Yuan, S. Zhang, Chitosan/sodium polyborate based micro-nano coating with high flame retardancy and superhydrophobicity for cotton fabric, Int. J. Biol. Macromol. 205 (2022) 261–273.
[12] Z. Miao, D. Yan, T. Zhang, F. Yang, S. Zhang, W. Liu, Z. Wu, High-efficiency flame retardants of a P-N-rich polyphosphazene elastomer nanocoating on cotton fabric, ACS Appl. Mater. Interfaces 13 (27) (2021) 32094–32105.
[13] B. Lin, A.C.Y. Yuen, T.B.Y. Chen, B. Yu, W. Yang, J. Zhang, Y. Yao, S. Wu, C. H. Wang, G.H. Yeoh, Experimental and numerical perspective on the fire performance of MXene/Chitosan/Phytic acid coated flexible polyurethane foam, Sci. Rep. 11 (1) (2021) 4684.
[14] X.-W. Cheng, J.-P. Guan, X.-H. Yang, R.-C. Tang, F. Yao, A bio-resourced phytic acid/chitosan polyelectrolyte complex for the flame retardant treatment of wool fabric, J. Clean. Prod. 223 (2019) 342–349.
[15] Y. Fang, J. Wu, Y.W.L. Chen, Durable flame retardant and anti-dripping of PET fabric using bio-based covalent crosslinking intumescent system of chitosan and phytic acid, Prog. Org. Coat. 183 (2023) 107785.
[16] Y. Fang, D.W.L. Qi, Flame retardant cotton fabrics with ultra-fast and long-term fire early warning response, Int. J. Biol. Macromol. 271 (2024) 132673.
[17] P. Li, B. Wang, Y.-J. Xu, Z. Jiang, C. Dong, Y. Liu, P. Zhu, Ecofriendly flame-retardant cotton fabrics: preparation, flame retardancy, thermal degradation properties, and mechanism, ACS Sustain. Chem. Eng. 7 (23) (2019) 19246–19256.
[18] C. Mo, L. Xiang, Y. Chen, Advances in injectable and self-healing polysaccharide hydrogel based on the Schiff base reaction, Macromol. Rapid Commun. 42 (10) (2021) 2100025.
[19] S. Li, M. Pei, T. Wan, H. Yang, S. Gu, Y. Tao, X. Liu, Y. Zhou, W. Xu, P. Xiao, Self-healing hyaluronic acid hydrogels based on dynamic Schiff base linkages as biomaterials, Carbohydr. Polym. 250 (2020) 116922.
[20] Y. Li, Y. Wu, K. Li, H. Lin, M. Wang, L. Zheng, C. Wu, X. Zhang, Recycling of epoxy resins with degradable structures or dynamic cross-linking networks: a review, Ind. Eng. Chem. Res. 63 (12) (2024) 5005–5027.
[21] F.C. Klein, M. Vogt, V. Abetz, Reprocessable vanillin-based schiff base vitrimers: tuning mechanical and thermomechanical properties by network design, Macromol. Mater. Eng. 309 (3) (2024) 2300187.
[22] P. Zamani, O. Zabihi, M. Ahmadi, M.R. Zamani, M.J. Zohuriaan-Mehr, T. Kannangara, P. Joseph, M. Naebe, Assessing sustainability and green chemistry in synthesis of a Vanillin-based vitrimer at scale: enabling sustainable manufacturing of recyclable carbon fiber composites, Compos. A Appl. Sci. Manuf. 179 (2024) 108016.
[23] S.M.A.S. Keshk, A.M. Ramadan, S. Bondock, Physicochemical characterization of novel Schiff bases derived from developed bacterial cellulose 2,3-dialdehyde, Carbohydr. Polym. 127 (2015) 246–251.
[24] E.H. Cordes, W.P. Jencks, The mechanism of hydrolysis of schiff bases derived from aliphatic amines, J. Am. Chem. Soc. 85 (18) (1963) 2843–2848.
[25] R. Nayak, J. Halder, T.K. Rajwar, D. Pradhan, V.K. Rai, D. Dubey, B. Kar, G. Ghosh, G. Rath, Metronidazole loaded chitosan–phytic acid polyelectrolyte complex nanoparticles as mucoadhesive vaginal delivery system for bacterial vaginosis, Int. J. Biol. Macromol. 255 (2024) 128212.
[26] S. Hasanvand, B. Ebrahimi, G. Paimard, M. Rouhi, Z. Hashami, R. Zibaei, Z. Roshandel, R. Mohammadi, Optimization of Seleno-chitosan-phytic acid nanocomplex for efficient removal of patulin from apple juice, Food Chem. 443 (2024) 138576.
[27] X. Yang, G. Yin, Z. Li, P. Wu, X. Jin, Q. Li, The preparation and chemical structure analysis of novel POSS-based porous materials, Materials 12 (12) (2019) 1954.
[28] F. Kholiya, J.P. Chaudhary, N. Vadodariya, R. Meena, Synthesis of bio-based aldehyde from seaweed polysaccharide and its interaction with bovine serum albumin, Carbohydr. Polym. 150 (2016) 278–285.
[29] M.N. Prabhakar, G.M. Raghavendra, B.V.D. Vijaykumar, K. Patil, J. Seo, S. Jung-il, Synthesis of a novel compound based on chitosan and ammonium polyphosphate for flame retardancy applications, Cellul. 26 (16) (2019) 8801–8812.
[30] Q. Zhao, X. Cheng, J. Kang, L. Kong, X. Zhao, X. He, J. Li, Polyvinyl alcohol flame retardant film based on halloysite nanotubes, chitosan and phytic acid with strong mechanical and anti-ultraviolet properties, Int. J. Biol. Macromol. 246 (2023) 125682.
[31] C. Yang, J. Liu, P. Liu, W. Wang, H. Chen, L. Bai, H. Yang, L. Yang, D. Wei, Phytic acid extracted cellulose nanocrystals for designing self-healing and anti-freezing hydrogels' flexible sensor, Chem. Eng. J. 493 (2024) 152276.
[32] H.-B. Yuan, R.-C.-B. Tang, Flame retardant functionalization of microcrystalline cellulose by phosphorylation reaction with phytic acid, Int. J. Mol. Sci. 22 (17) (2021) 9631.
[33] Y. Ning, R. Liu, W. Chi, X. An, Q. Zhu, S. Xu, L. Wang, A chitosan derivative/phytic acid polyelectrolyte complex endowing polyvinyl alcohol film with high barrier, flame-retardant, and antibacterial effects, Int. J. Biol. Macromol. 259 (2024) 129240.
[34] G. Wang, H. Li, Y. Shao, X. Wu, Q. He, K. Niu, Preparation method of biogenic phytic acid and chitosan-related epoxy resin flame retardant: a review, J. Polym. Res. 30 (7) (2023) 269.
[35] F. Carosio, J. Alongi, G. Malucelli, Layer by Layer ammonium polyphosphate-based coatings for flame retardancy of polyester–cotton blends, Carbohydr. Polym. 88 (4) (2012) 1460–1469.
[36] J.-w. Gu, G.-c. Zhang, S.-l. Dong, Q.-Y. Zhang, J. Kong, Study on preparation and fire-retardant mechanism analysis of intumescent flame-retardant coatings, Surf. Coat. Technol. 201 (18) (2007) 7835–7841.
[37] C. Fu, X. Xu, G.-Z. Yin, B. Xu, P. Li, B. Ai, Z. Zhai, F. Gao, J. Zhai, D.-Y. Wang, Surface engineering for cellulose as a boosted Layer-by-Layer assembly: excellent flame retardancy and improved durability with introduction of bio-based "molecular glue", Appl. Surf. Sci. 585 (2022) 152550.
[38] Q. Jiang, P. Li, Y. Liu, P. Zhu, Phytic acid-iron/laponite coatings for enhanced flame retardancy, antidripping and mechanical properties of flexible polyurethane foam, Int. J. Mol. Sci. 23 (16) (2022) 9145.
[39] Y. Chen, N. Yin, Y. Wang, S. Gao, C. Shen, A novel bio-based charcoal-forming agent based on chitosan and phytate@Mg to improve the flame retardancy of poly (lactic acid), J. Appl. Polym. Sci. 141 (11) (2024) e55074.
[40] P. Li, C. Liu, Y.-J. Xu, Z.-M. Jiang, Y. Liu, P. Zhu, Novel and eco-friendly flame-retardant cotton fabrics with lignosulfonate and chitosan through LbL: Flame retardancy, smoke suppression and flame-retardant mechanism, Polym. Degrad. Stab. 181 (2020) 109302.
[41] J. Li, W. Jiang, M. Liu, Durable phosphorus/nitrogen flame retardant for cotton fabric, Cellul. 29 (8) (2022) 4725–4751.
[42] Y. Feng, Y. Zhou, D. Li, S. He, F. Zhang, G. Zhang, A plant-based reactive ammonium phytate for use as a flame-retardant for cotton fabric, Carbohydr. Polym. 175 (2017) 636–644.
[43] A.-N. Zhang, H.-B. Zhao, J.-B. Cheng, M.-E. Li, S.-L. Li, M. Cao, Y.-Z. Wang, Construction of durable eco-friendly biomass-based flame-retardant coating for cotton fabrics, Chem. Eng. J. 410 (2021) 128361.
[44] W. Rao, J. Shi, C. Yu, H.-B. Zhao, Y.-Z. Wang, Highly efficient, transparent, and environment-friendly flame-retardant coating for cotton fabric, Chem. Eng. J. 424 (2021) 130556.
[45] J. Li, W. Jiang, Synthesis of a novel P-N flame retardant for preparing flame retardant and durable cotton fabric, Ind. Crop. Prod. 174 (2021) 114205.
[46] X. Luo, Z. Li, J. Shen, L. Liu, H. Chen, Z. Hu, I. Krucinska, J. Yao, A facile strategy to achieve efficient flame-retardant cotton fabric with durable and restorable fire resistance, Chem. Eng. J. 430 (2022) 132854.
[47] X. Cheng, L. Shi, Z. Fan, Y. Yu, R. Liu, Bio-based coating of phytic acid, chitosan, and biochar for flame-retardant cotton fabrics, Polym. Degrad. Stab. 199 (2022) 109898.